ISBN: 978-3-95450-247-9 ISSN: 2673-5490 doi: 10.18429/JACoW-IPAC2024-THPG71

COMMISSIONING OF THE DIGITAL LLRF SYSTEM AT THE KEK PHOTON FACTORY 2.5 GeV RING*

D. Naito†, N. Yamamoto, T. Takahashi, A. Motomura, S. Sakanaka
Accelerator Laboratory, High Energy Accelerator Research Organization(KEK), Tsukuba, Japan

Abstract

The LLRF system of the KEK-PF 2.5 GeV ring was replaced in 2023. The old LLRF system is a conventional analog system, whereas the new system is an FPGA-based digital system. The commissioning of the new LLRF system was carried out in early November where the feedback parameters were optimized. Then, the new system was successfully used for three months in user operations. The amplitude and phase variations of the cavity voltage were within ±0.06% and ±0.06°, respectively, at the nominal beam current of 450 mA. In this paper, we introduce our new system and report on the commissioning results.

INTRODUCTION

A low-level RF (LLRF) system of the KEK Photon Factory 2.5 GeV ring (PF ring) [1] was replaced by an FPGA-based digital LLRF system in order to improve maintainability and performance. The new system is composed of digital boards based on the MTCA.4 standard [2]. In this paper, we introduce our new LLRF system and its features. We also report on the commissioning results of the new LLRF system with the stored beam.

NEW LLRF SYSTEM

The new LLRF system [3] is composed of one Micro TCA Carrier Hub (MCH), six pairs of Advanced Mezzanine Card (AMC) and Micro Rear Transition Module (μRTM), and one Extended Rear Transition Module (eRTM). The MCH mediates the EPICS communications between the AMCs and an operation server. A single pair of AMC and μRTM controls a single RF station which includes a cavity and a klystron.

Table 1 shows principal parameters of the RF system. The PF ring has totally four RF stations, and the four pairs of boards, called LLRF boards, are used for RF control. The remaining two pairs, called fast interlock (FITL) boards, monitor reflected signals from two RF stations per pair. When the amplitude of a reflected signal exceeds an interlock threshold, the FITL board sends the RF off signal to the LLRF boards via M-LVDS lines. These AMC and μRTM were developed by customizing the LLRF technologies established at the J-PARC [4].

The eRTM board generates the clock signal and distributes it to each AMC via the RF backplane. The eRTM also distributes the master RF signal to an IQ modulator located on the μRTM. The frequency of the clock and the master RF are 307.75 MHz and 500.1 MHz, respectively. We used the eRTM developed at the SPring-8 [5].

Table 1: The Principal Parameters of the RF System for the Photon Factory Storage Ring

Parameter	Value
Number of cavities	4
Radio frequency	500.1 MHz
Harmonic number	312
Cavity voltage per cavity	0.425 MV
Beam current	450 mA
Klystron power per cavity	72 kW

RF CONTROL SCHEME AND ITS FEATURES

Figure 1 shows the block diagram of the RF control in the new LLRF system. The RF control is implemented in the FPGA, and it is controlled via the EPICS communications. We adopted double feedback loops, that are, the cavity input and cavity pickup feedbacks. An output signal from the cavity pickup feedback is used as a reference signal for the cavity input feedback. By setting a different bandwidth for each feedback loop, we distinguish the compensation target of each feedback. The cavity input feedback stabilizes the RF wave that are input to the cavity. Fluctuations in the RF wave are primarily caused by ripples in the power supply for the klystrons; the frequency of the ripples observed at our power supply was less than 10 kHz. The cavity pickup feedback compensates for the variation induced by tuning error and beam loading; the frequency of these variation is typically several Hz. Considering the frequencies of these disturbances, the bandwidth of the cavity input and cavity pickup feedbacks were initially set to 10 kHz and 20 Hz, respectively, where the bandwidth was determined by an IIR filter that located in front of each feedback controller. The feasibility of this double-loop scheme has been demonstrated at the SPring-8 [5].

Both the cavity input and pickup signals are input to ADCs, and they are sampled directly. The frequency of the signals and the sampling are 500.1 MHz and 307.75 MHz, respectively. The digital signals are then converted to the IQ signals by the non-IQ sampling method [6]. To eliminate high-frequency noises associated with the ADC sampling, the IQ signals pass through an IIR filter having a cutoff frequency of 100 kHz. The filtered signals are converted to amplitude and phase, which are independently controlled by

* Work supported by JSPS KAKENHI Grant Numbers JP20H04459, JP24K03210 and JP24K15601.
† daichi.naito@kek.jp

ISBN: 978-3-95450-247-9 ISSN: 2673-5490 doi: 10.18429/JACoW-IPAC2024-THPG71

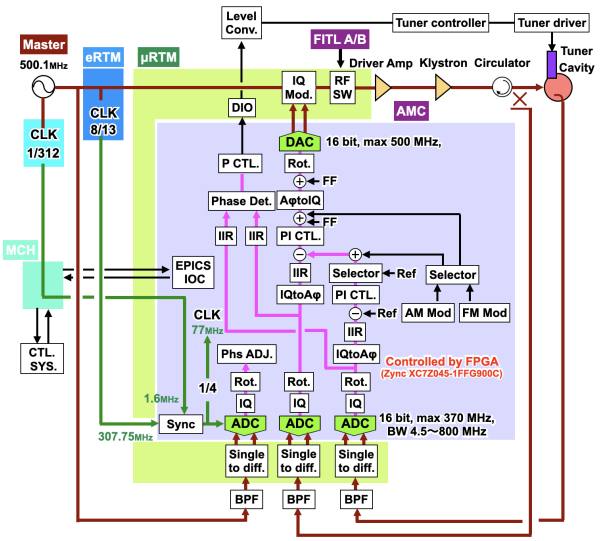

Figure 1: The block diagram of the RF control in the new LLRF system. [3].

proportional and integral feedback controllers indicated by "PI CTL." in Fig. 1.

The feature of our RF control scheme is that the sampling frequency of the ADC is set to be 8/13 (307.75 MHz) of the RF frequency, where the denominator (13) is the divisor of the harmonic number (312) of the storage ring. This allows us to detect the transient variation of the cavity voltage that is synchronized with the beam revolution. This function will be useful for compensating the transient beam-loading effect in double RF systems for synchrotron light sources [7].

INSTALLATION AND COMMISSIONING

The new LLRF system was installed in the PF ring in July 2023. We evaluated its performance and adjusted the feedback parameters of RF control without stored beam [3]. In early November 2023, we carried out the beam commissioning of the LLRF system by three steps.

The first step was to adjust the RF phase of each cavity so that the electron bunches receive the maximum RF voltage. This adjustment was carried out at beam current of 20 mA. After the adjustment, observed synchrotron frequency was 23.2 kHz which agreed with a calculated synchrotron frequency of 23.5 kHz at an RF voltage of 1.7 MHz. The current of the stored beam was then increased.

The second step was to adjust the feedback parameters at high beam current. When the beam current exceeded 100 mA, signal oscillation suddenly occurred in the feedback loop, and then, the output of the LLRF was turned off by the interlock due to a reflected power from the cavity. To avoid this feedback oscillation, we adjusted the bandwidth of the cavity pickup feedback by changing the cutoff frequency of the IIR filter used in the cavity pickup feedback. Figure 2 shows the maximum beam current achieved without any feedback oscillations as a function of the IIR-filter cutoff frequency. By increasing the cutoff frequency from 20 Hz

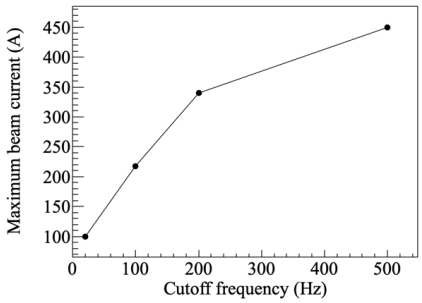

Figure 2: Maximum beam current achieved without any feedback oscillations as a function of the IIR-filter cutoff frequency.

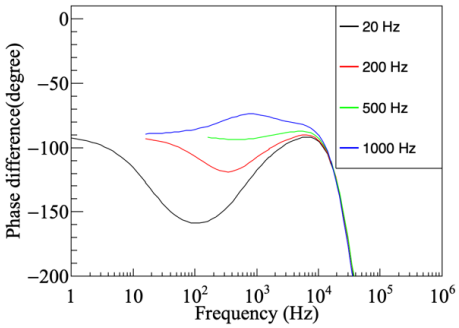

Figure 3: Phase difference between the input and output of the cavity-pickup feedback controller as a function of the frequency. A simplified simulation without beam.

to 500 Hz, we successfully stored the beam current of 450 mA, that is, a nominal beam current for user operations.

Before the commissioning, we conducted a simple simulation on our double-feedback loops using MATLAB/Simulink software [8]. In this simulation, we modeled the klystron and the cavity by low-pass filters, and we did not include the effect of beam. Figure 3 shows a result of simulations where the phase difference between the input and output of the cavity pickup feedback controller is indicated as a function of frequency. The horizontal and vertical axes show the input signal frequency and the phase difference, respectively. Four traces in Fig. 3 indicate the phase differences when the cutoff frequency for the cavity pickup feedback is set to be 20 Hz, 200 Hz, 500 Hz, and 1 kHz, respectively. When the cutoff frequency is low, a downward peak in the phase difference appeared. If the phase difference, shown in Fig. 3, falls below -180 degrees and the gain between the input and output of the cavity-pickup feedback controller exceeds 0 dB, the feedback system becomes unstable. This simulation suggests that our double feedback system is prone to be unstable when the cutoff frequency of the cavity pickup loop is set to be as low as 20–200 Hz.

Figure 4 shows the frequency of the feedback oscillation (black points) observed under beam operations and the frequency of downward peaks (red points) observed in simulations as a function of the cutoff frequency. Both the

ISBN: 978-3-95450-247-9 ISSN: 2673-5490 doi: 10.18429/JACoW-IPAC2024-THPG71

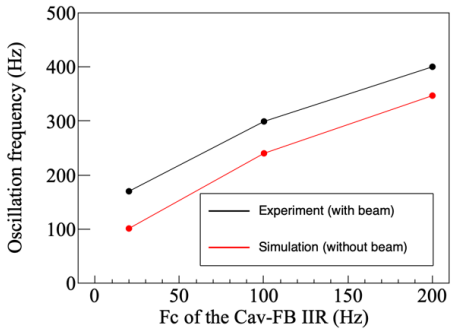

Figure 4: The frequency of the feedback oscillation as a function of the cutoff frequency.

feedback-oscillation frequency (black points) and the peak frequency (red points) depended on the cutoff frequency in a similar trend. We presume that under high beam current, the double feedback system became unstable due to some effect of beam, and that the feedback system became stabilized by increasing the cutoff frequency.

The third step was to optimize the gain of the cavity pickup feedback. This was done to maximize the stability of the cavity voltage at the beam current of 450 mA. The proportional and integral gains of the cavity pickup feedback were scanned step by step until the oscillation occurred in the feedback. Figure 5 shows the amplitude variation of the cavity pickup signal as a function of the feedback parameters, whereas Fig. 6 shows the similar data without beam. The horizontal and vertical axes show the set values of the proportional and integral gains, respectively. The amplitude variation, indicated by color bars in Figs. 5 and 6, is defined by the RMS value of the amplitude fluctuation divided by the mean amplitude. In Fig. 5, the blank (white) region represents the region where the RF was turned off by the feedback oscillation.

Looking at Figs. 5 and 6, we can see two features: 1) the stable region is extremely narrow with beam as compared that without beam, and 2) the amplitude variation was larger with beam. For example, the amplitude variation around the operation point is approximately 0.06 %, which is higher by 5 times as compared to that without beam. As shown in Fig. 5, we changed the operation point, that is a pair of proportional and integral gains, from (2, 7.3e3) to (1, 2.9e3). After this optimization, the amplitude and phase variations of the cavity voltage became within ±0.056% and ±0.053°, respectively, at the beam current of 450 mA. The new LLRF system then achieved an excellent performance.

SUMMARY

In July 2023, the digital LLRF system based on the MTCA.4 standard was installed in the PF 2.5 GeV ring. After its performance tests, we carried out the commissioning of the LLRF system with beam. First, the phase difference of the RF between four cavities was adjusted to provide the maximum RF voltage. Second, we adjusted the cutoff frequency of the IIR filter for the cavity pickup feedback to prevent the feedback oscillation. Third, the gain parameters of the cavity pickup feedback were optimized. As a result, we achieved an excellent stability of the cavity voltage; the variation of the amplitude and phase were within ±0.056% and ±0.053°, respectively, at the nominal beam current of 450 mA. During these studies, we found that the performance of the feedback control decreased under high beam current. We plan to investigate this by means of beam studies and advanced simulations.

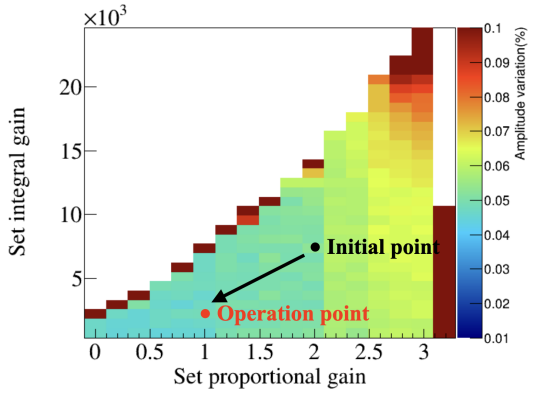

Figure 5: Measured amplitude variation of the cavity pickup signal as the function of the feedback parameters with a beam current of 450 mA.

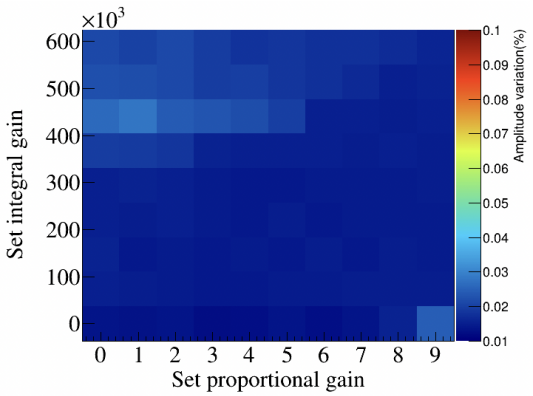

Figure 6: Measured amplitude variation of the cavity pickup signal as the function of the feedback parameters without the beam. Note that the scales in horizontal and vertical axes are larger as compared to those in Fig. 5.

ACKNOWLEDGEMENT

We thank the following staff of Mitsubishi Electric Defense and Space Technologies corporation for their dedication to producing the new LLRF system: T. Iwaki, R. Kitagawa, A. Terada, T. Harigae, S. Yamazaki, T. Okochi, and M. Ryoshi. We are also grateful to T. Ohshima (SPring-8), F. Tamura (JAEA), T. Kobayashi, Y. Sugiyama, K. Futatsukawa, T. Matsumoto, T. Miura (all of KEK) for useful information and discussions.

ISBN: 978-3-95450-247-9 ISSN: 2673-5490 doi: 10.18429/JACoW-IPAC2024-THPG71

REFERENCES

[1] M. Izawa, S. Sakanaka, T. Takahashi, and K. Umemori, "Present Status of the Photon Factory RF System", in *Proc. APAC'04*, Gyeongju, Korea, Mar. 2004, paper TUP14016, pp. 389–391. http://accelconf.web.cern.ch/accelconf/a04/PAPERS/TUP14016.PDF

[2] PICMG, "MicroTCA Overview"; https://www.picmg.org/openstandards/microtca/

[3] D. Naito, N. Yamamoto, T. Takahashi, M. Motomura, and S. Sakanaka, "LLRF upgrade status at the KEK Photon Factory 2.5 GeV ring", in *Proc. LLRF23*, Gyeongju, Korea, Oct. 2023. doi:10.48550/arXiv.2310.13970

[4] F. Tamura, Y. Sugiyama, M. Yoshii, and M. Ryoshi, "Development of Next-Generation LLRF Control System for J-PARC Rapid Cycling Synchrotron", in *Proc. IEEE TNS*, vol. 66, no. 7, July. 2019, pp. 1242–1248. doi:10.1109/TNS.2019.2899358

[5] T. Ohshima *et al.*, "Development of a New LLRF System Based on MicroTCA.4 for the SPring-8 Storage Ring", in *Proc. PASJ'18*, Nagaoka, Japan, Aug. 2018, paper WEOL10, pp. 55–59. [in Japanese]. https://www.pasj.jp/web_publish/pasj2018/proceedings/PDF/WEOL/WEOL10.pdf

[6] T. Schilcher, "RF applications in digital signal processing", CERN, Geneva, Switzerland, in Rep. CERN-2008-003, May. 2007, pp. 249–283.

[7] N. Yamamoto, T. Takahashi, and S. Sakanaka, "Reduction and compensation of the transient beam loading effect in a double rf system of synchrotron light sources", *Phys. Rev. Accel. Beams*, vol 21, no. 1, p. 012001, Jan. 2018. doi:10.1103/PhysRevAccelBeams.21.012001

[8] MATLAB/Simulink by The MathWorks, Inc., https://jp.mathworks.com